

Laser stimulated nonlinear optics of Ag nanoparticle-loaded poriferous TiO₂ microtablet

S. NAFISAH¹, S.K.M. SAAD¹, A.A. UMAR¹, K. PLUCINSKI^{2*},
M. LIS³, A. MACIAGA³, R. MIEDZINSKI⁴

¹Institute of Microengineering and Nanoelectronic (IMEN), Universiti Kebangsaan Malaysia, 43600 Bangi, Selangor, Malaysia

²Institute of Electronics, Military University of Technology, Kaliskiego 2, 00-908 Warsaw, Poland

³Faculty of Electrical Engineering, Częstochowa University of Technology, Armii Krajowej 17, 42-200 Częstochowa, Poland

⁴Institute of Physics, Jan Długosz University in Częstochowa, Armii Krajowej 13/15, 42-200 Częstochowa, Poland

*Corresponding author: kpluc2006@wp.pl

The studies of the photoinduced second harmonic generation were performed for the Ag-loaded poriferous TiO₂ microtablets deposited on an ITO substrate. The poriferous TiO₂ microtablets on a pre-cleaned ITO substrate (Kaivo, China, sheet resistance of *ca.* 10 Ω/square) were prepared by simply immersing the ITO substrate vertically into the growth solution that contains 5 ml of 0.5 M (NH₄)₂TiF₆ (Sigma-Aldrich) and 5 ml of 1.0 M H₃BO₃ (R.M. Chemicals) for 15 h at room temperature. The samples were obtained from the growth solution with concentration of 0.4, 0.5 and 0.6 M. We have found that maximal second harmonic generation signal was achieved for the samples with concentration 0.5 M.

Keywords: Ag-loaded poriferous TiO₂ microtablets, photoinduced second harmonic generation.

1. Introduction

The studies of photoinduced nonlinear optical effects in different disordered solid states present an important topic of modern optoelectronic and nonlinear optics [1].

Among the disordered materials are the nanocomposites which are very promising candidates that possess highly localized states contributing to the corresponding nonlinear optical constants [2]. The morphology of interfaces defining the corresponding nonlinear optical constants as well as the local dielectric fields play the principal

role. The phonon states which effectively interact with the trapping levels play an additional role [3].

Among the disordered materials very crucial are the sol-gel materials [4]. The considered materials were used first of all as holographic materials. In [5] the photoinduced second-order susceptibility of germanosilicate glasses on the GeO_2 - SiO_2 composition was explored by a coherent superposition of coherent 800-nm fundamental and 400-nm doubled frequency light of a femtosecond laser. It was established that laser-stimulated optical nonlinearity increased with increasing GeO_2 content. Photoinduced picosecond nonlinear optics was in details explored in [6]. The role of the picosecond Raman scattering is studied. The infrared stimulated second harmonic generation (SHG) was also discovered in the chalcogenide glasses [7] and the principal role of the anharmonic phonons was found. The photoinduced SHG was substantially enhanced in the nanocrystallites [8, 9] and the principal role here plays the flattening of the bands [10], multi-photon processes [11], partial crystallization [12].

Moreover, these materials do not possess such high SHG efficiency as traditional inorganic crystals [13]. They allow to perform the continuous tuning of their susceptibilities. The simultaneous presence of semiconductor and silver nanoparticles may be very promising for this goal.

In the present work we develop a novel technique of synthesizing TiO_2 nanoparticles with the aim to use these nanoparticles as promising materials in photoinduced nonlinear optics.

2. Experiment

2.1. Ag-loaded porous TiO_2 microtablet preparation

Ag-loaded porous TiO_2 microtablets (Ag-PTM) on an ITO substrate were prepared by a two-step process, *i.e.*, PTM growth and Ag nanoparticle loading onto the PTMs structure. The PTMs were prepared by using our previously reported technique, namely a liquid phase deposition [14, 15]. Briefly, the PTMs on a pre-cleaned ITO substrate (Kaivo, China, sheet resistance of *ca.* 10 Ω /square) were prepared by simply immersing the ITO substrate vertically into the growth solution that contains 5 ml of 0.5 M $(\text{NH}_4)_2\text{TiF}_6$ (Sigma-Aldrich) and 5 ml of 1.0 M H_3BO_3 (R.M. Chemicals) for 15 h at room temperature. The PTMs-coated ITO was then taken out from the growth solution and washed using a copious amount of pure water. After that, it was dried using a flow of nitrogen gas before being annealed for 1 h in air at 400°C using a split-tube furnace system (Thermcraft, USA). From this procedure, high-density PTMs structure on the ITO substrate with an anatase phase (confirmed by XRD result) will be obtained.

In this study, three different PTMs densities on the ITO substrate surface were synthesized by simply varying the Ti^+ precursor, *i.e.*, $(\text{NH}_4)_2\text{TiF}_6$, into three concentrations, namely 0.4, 0.5 and 0.6 M. Other reagents and the procedure were kept unchanged.

The Ag nanoparticle-loaded PTMs (Ag-PTMs) were prepared by firstly immersing the PTM-coated ITO substrate into a 20 ml aqueous solution that contains 0.5 ml of 0.01 M AgNO₃ (Sigma-Aldrich) and 0.5 ml of 0.01 M trisodium citrate (WAKO Chemical) [16–18]. The sample was kept undisturbed for 30 min. Then, a 0.1 ml of ice-cooled NaBH₄ (0.1 M) was injected into the solution. At this stage, the solution color changed from colorless to yellow, indicating the formation of Ag nanoparticles both in the solution and on the PTMs surface. After that, the sample was taken out from the solution, washed with pure water and then dried with a flow of nitrogen gas. Finally, the sample was annealed in air at 200°C for 1 h to remove any organic residue.

2.2. Characterizations

The morphologies of the unloaded and Ag-loaded PTMs were obtained using a field emission scanning electron microscopy (FESEM) ZEISS SUPRA 55VP FESEM apparatus. The dimension and the surface growth density of the PTMs were obtained from the ImageJ software analysis. The phase and the structural property of the unloaded and Ag-loaded PTMs were characterized by X-ray diffraction (XRD) measurements using a Bruker D8 Advance apparatus with CuK α irradiation ($\lambda = 1.541 \text{ \AA}$). The optical absorption of the PTM was collected using a UV–vis spectrophotometer (Lambda 900 Perkin Elmer) with spectral resolution 0.5 nm.

3. Results and discussion

Poriferous TiO₂ microtablets (PTMs) with three different surface densities have been successfully prepared on the ITO substrate that was achieved by simply varying the concentration of the growth solution. Figures 1a–1c shows the typical FESEM image of the PTMs that was obtained from the growth solution with concentration of 0.4, 0.5 and 0.6 M (see Section 2 for detailed information of the growth solution). As can be seen from Figs. 1a–1c, the PTMs have been effectively grown on and covered the substrate surface with their density increasing with the increase in the growth solution concentration. As also can be seen from the image, the PTMs prepared using the lower growth solution concentration (see Fig. 1a) produce dispersed PTMs. However, at high growth solution concentration, high-density and highly overlapped PTMs were obtained. According to the ImageJ software analysis, the PTMs surface densities were estimated to be approximately 5, 20 and 150 PTMs/10 μm^2 for the samples prepared using the growth solution of 0.4, 0.5 and 0.6 M, respectively. As Fig. 1a shows, the PTMs feature morphology is of circular shape. Nevertheless, in some cases, PTMs with quasi-square morphology were also obtained. The diameter of the PTMs is ranging from 5 to 15 μm . Meanwhile, the thickness is ranging from 1 to 3 μm . It was observed that the dimension of the PTMs seems to be independent of the growth solution concentration used. As has been mentioned previously, the growth solution concentration only influences the surface density of the PTMs growth.

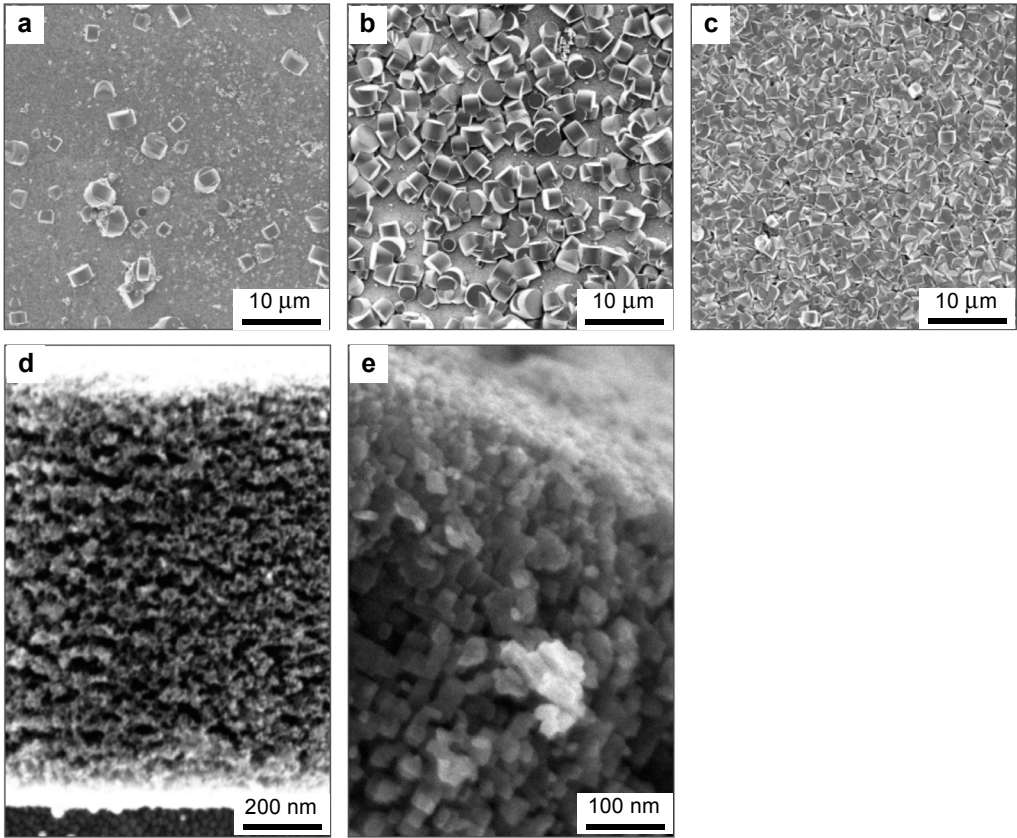


Fig. 1. FESEM micrograph for PTMs with different surface density prepared using different concentration of Ti^+ precursor molarities, namely 0.4 M (a), 0.5 M (b) and 0.6 M (c) of $(\text{NH}_4)_2$. High-resolution FESEM image of the surface (d) and inner side (e) structures of the PTMs.

While Figs. 1a–1c show the growth characteristics and dispersion of the PTMs on the surface, Figs. 1d and 1e show a detailed structure of the PTMs, *i.e.*, the surface and the inner side structures. As can be seen from the image, the PTMs surface is decorated by small nanowires of dimension approximately 200 and 100 nm in length and diameter. Meanwhile, the inner structure of the PTMs is constructed by nanocuboids that are arranged in a brick-like formation. The nanocuboids width, length and thickness are approximately 10, 20 and 5 nm, respectively.

The PTMs growth on the surface with unique surface distribution as well as its peculiar individual structure with hairy surface and poriferous and being constructed by nanocuboid in the inner structure may promise distinguished optical properties to be used in linear and nonlinear optical applications [16–22].

Figure 2 shows the typical higher resolution FESEM image of the PTMs of different surface densities as shown in Fig. 1 that are loaded with Ag nanoparticles. As

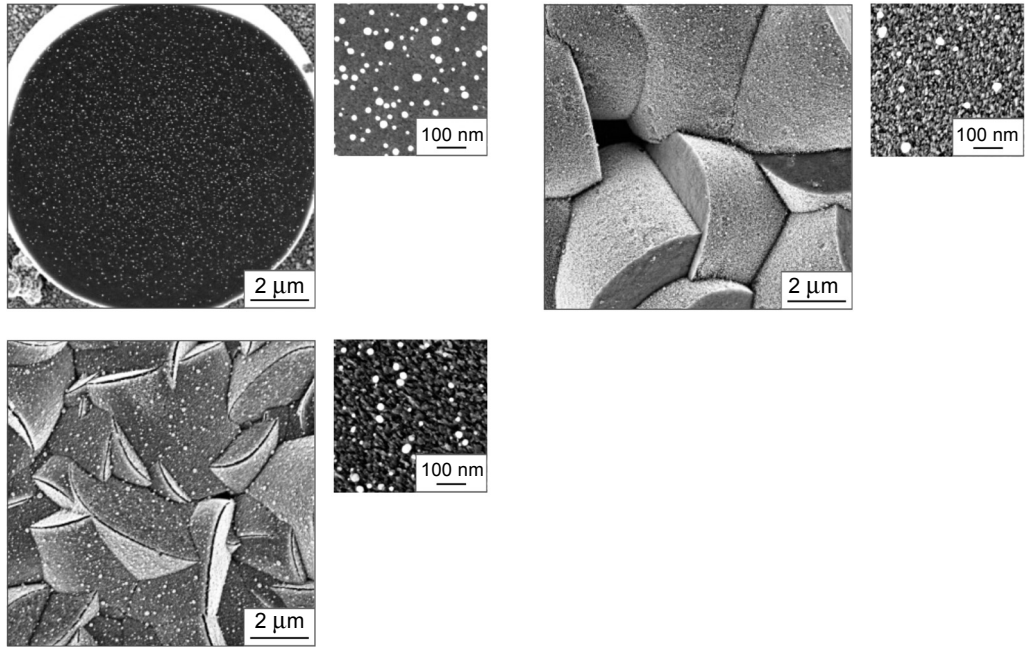


Fig. 2. FESEM images of PTMs with three different surface densities loaded with Ag nanoparticles. Inset figures are the related high-resolution image of the PTMs surface showing Ag nanoparticles (bright spot).

Figure 2 shows, the Ag nanoparticles have been successfully attached onto the PTMs structure. The Ag nanoparticles are indicated with the spherical bright spots (see white circle). It was observed that the Ag nanoparticles are well-dispersed on the surface of PTMs without the presence of aggregation amongst them. This condition may preserve the unique localized-plasmon resonance properties of the Ag, which may be potentially used in optical applications. The size of Ag nanoparticle is in the range of 15–40. Because the Ag nanoparticles size is larger than the size of the nanowires decorating the PTMs surface, Ag nanoparticles are indeed attached on the tip of the nanowires. This condition may further promise novel optical properties due to having a nanostructured substrate of nanowires of TiO_2 . Thus, unusual linear and nonlinear optical effects are expected to be produced from this system.

While FESEM image in Figs. 1 and 2 confirm the formation of PTMs and Ag nanoparticle-loaded PTMs, the X-ray diffraction spectrum further proves the formation of Ag nanoparticles-loaded PTMs phase on the ITO substrate surface. The result is shown in Fig. 3. As Figure 3 shows, seven diffraction peaks, namely at 2θ of 25, 37, 38.2, 46, 47.5, 54 and 56 deg are observed in the spectrum along with the peaks attributed to the ITO substrate. According to the JCPDS file no. 21-1272, the peaks at 2θ of 25, 37, 47.5, 54 and 56 deg can be associated with the Bragg planes of (101), (004), (200), (105) and (215) anatase TiO_2 , respectively. Meanwhile, the diffraction peak at 2θ of 38.2 and 46 deg can be related to the (111) and (200) planes of *fcc* Ag nanoparticles

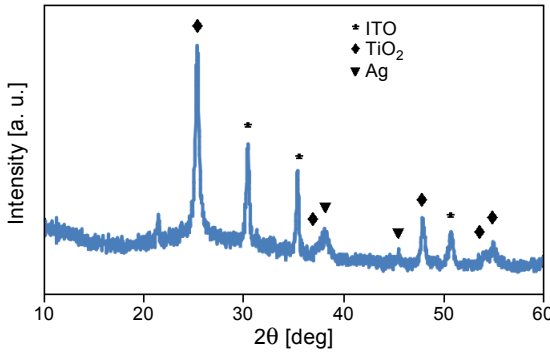


Fig. 3. Typical XRD spectrum of Ag nanoparticle-loaded PTMs.

(judging from the JCPDS file no. 04-0783). Thus, these results confirm the formation of Ag and TiO₂ nanocrystalline phases on the substrate surface. Moreover, on the Ag nanoparticles diffraction peaks, as can be seen from the figure, they are relatively small compared to the TiO₂. This could be related to the small crystallite size of the Ag nanoparticles, which is also confirmed by the FESEM image as shown in Fig. 2. Such small crystallite size seemed to be further confirmed by the UV–vis optical absorption spectra of the samples, indicating the presence of small surface plasmonic character of the Ag nanoparticles.

Optical absorption spectroscopy has been carried out on the sample. The result is shown in Fig. 4. As can be seen from the curves, the spectra are dominated by the TiO₂ layer profile. It can be related to the high thickness of the PTMs on the surface. Thus, light scattering by the PTMs is relatively high. In spite of that fact, the profile of surface plasmon resonance of the Ag nanoparticle can be recognized from the curves, which is located approximately at 475 nm. This is because the light scattering is too high as the result of large thickness of the PTMs on the surface. This effect is much pronounced at the higher surface density of PTMs (see curves *b* and *c*). Despite a low signal of Ag nanoparticle surface plasmon resonance (SPR) recorded by the UV–vis

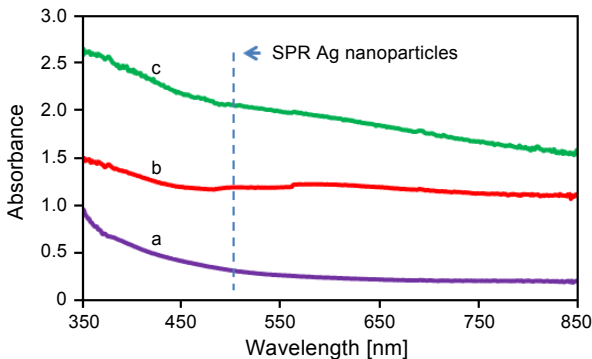


Fig. 4. UV–vis spectra of Ag nanoparticle-loaded PTMs. Dashed-line indicating the position of SPR character of Ag nanoparticles (see text for explanation).

spectroscopy technique, unusual SHG may probably be obtained from the system due to the unique composite structure of Ag nanoparticles and PTMs on the substrate surface.

The photoinduced SHG was measured similarly to the described in [23]. The corresponding results are presented in Fig. 5.

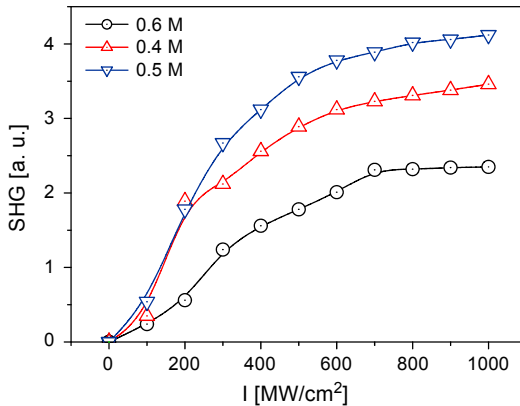


Fig. 5. Dependence of the optical second harmonic generation vs. the photoinduced power density.

Following Fig. 5, it was shown that the samples with 0.5 M demonstrate the maximal values of the photoinduced SHG. To avoid substantial inaccuracy, the measurements were performed for many points along the sample's surfaces. It was established that to achieve a good reproducibility of absorption, it is necessary to do the measurements at 50–60 points and for the SHG up to 150 points. So the SHG was more sensitive to the sample's nonhomogeneity. It should be added that the addition of silver favors the enhancement of the SHG up to 20%. This fact may be of great importance for the further optimization of the technology for production of the TiO₂ nanocomposites.

Following the obtained data, one can conclude that the studied materials may be promising for the optically operated triggering because the absolute increase in the SHG is up to 2 times.

4. Conclusions

The measurements of the photoinduced second harmonic generation were performed for the Ag-loaded porous TiO₂ microtablets (Ag-PTM) deposited on an ITO substrate. The PTMs on a pre-cleaned ITO substrate (Kaivo, China, sheet resistance of *ca.* 10 Ω/square) were prepared by simply immersing the ITO substrate vertically into the growth solution that contains 5 ml of 0.5 M (NH₄)₂TiF₆ (Sigma-Aldrich) and 5 ml of 1.0 M H₃BO₃ (R.M. Chemicals) for 15 h at room temperature. Thus, light scattering by the PTMs is relatively high. In spite of that fact, the profile of surface plasmon resonance of the Ag nanoparticle can be recognized from the curves, which is located approximately at 475 nm. This is because the light scattering is too high as the result

of large thickness of the PTMs on the surface. This effect is much pronounced at the higher surface density of PTMs (see curves *b* and *c*, Fig. 4). The samples were obtained from the growth solution with concentration of 0.4, 0.5 and 0.6 M. We have found that maximal SHG signal was achieved for the samples with concentration 0.5 M. This fact reflects a principal role for the nanointerfaces in the observed features [24]. The obtained results show the huge potential of the material as optical triggers.

References

- [1] KITYK I.V., GOLIS E., FILIPECKI J., WASYLAK J., ZACHARKO V.M., *Photoinduced nonlinear optical phenomena in PbO-BiO_{1.5}-GaO_{1.5} glass*, Journal of Materials Science Letters **14**(18), 1995, pp. 1292–1293.
- [2] EBOU THE J., KITYK I.V., BENET S., CLAUDET B., PLUCINSKI K.J., OZGA K., *Photoinduced effects in ZnO films deposited on MgO substrates*, Optics Communications **268**(2), 2006, pp. 269–272.
- [3] KITYK I.V., QINGSHENG LIU, ZHAOYONG SUN, JIYE FANG, *Low-temperature anomalies of two-photon absorption in In₂O₃ nanocrystals incorporated into PMMA matrixes*, The Journal of Physical Chemistry B **110**(16), 2006, pp. 8219–8222.
- [4] MARINO I.-G., RASCHELLÀ R., LOTTICI P.P., BERSANI D., RAZZETTI C., LORENZI A., MONTENERO A., *Photoinduced effects in hybrid sol-gel materials*, Journal of Sol-Gel Science and Technology **37**(3), 2006, pp. 201–206.
- [5] JINHAI SI, KANEHIRA S., MIURA K., HIRAO K., *Composition dependence of photoinduced second-order nonlinearity of germanosilicate glasses*, Optics Express **14**(10), 2006, pp. 4433–4438.
- [6] NESTEROVA Z.V., MELO MELCHOR G., ALEXANDROV I.V., *Medium-range ordering in glass structures as a background of photosensitivity in silica fibers*, Journal of Non-Crystalline Solids **351**(52–54), 2005, pp. 3789–3796.
- [7] GRUHN W., *Infrared second-order nonlinear optical effect in Sb₂Te₃-SrBr₂-PbCl₂ glass*, Optica Applicata **35**(3), 2005, pp. 329–338.
- [8] HEREST D., VOOLLESS F., *Manifestation of nano-sized effects in photoinduced nonlinear optics of CdI₂-Cu layered single crystals*, Optics and Lasers in Engineering **42**(1), 2004, pp. 85–89.
- [9] RAMTOLLI F., SACCINI G., *Nonlinear optical properties of ZnS nanocrystals incorporated within the polyvinyl alcohol photopolymer matrices*, Crystal Research and Technology **37**(12), 2002, pp. 1325–1330.
- [10] KITYK I.V., KASSIBA A., PLUCINSKI K., BERDOWSKI J., *Band structure of the large-sized SiC nanocomposites*, Physics Letters A **265**(5–6), 2000, pp. 403–410.
- [11] PLUCINSKI K.J., MAKOWSKA-JANUSIK M., MEFLEH A., KITYK I.V., YUSHANIN V.G., *SiON films deposited on Si(111) substrates – new promising materials for nonlinear optics*, Materials Science and Engineering B **64**(2), 1999, pp. 88–98.
- [12] MAJCHROWSKI A., KITYK I.V., ŁUKASIEWICZ T., MEFLEH A., BENET S., *CsLiB₆O₁₀ crystallites embedded into the olygoether photopolymer matrices as new materials for the acoustically induced nonlinear optics*, Optical Materials **15**(1), 2000, pp. 51–58.
- [13] PETROV V., GHOTBI M., KOKABEE O., ESTEBAN-MARTIN A., NOACK F., GAYDARDZHIEV A., NIKOLOV I., TZANKOV P., BUCHVAROV I., MIYATA K., MAJCHROWSKI A., KITYK I.V., ROTERMUND F., MICHALSKI E., EBRAHIM-ZADEH M., *Femtosecond nonlinear frequency conversion based on BiB₃O₆*, Laser and Photonics Reviews **4**(1), 2010, pp. 53–98.
- [14] UMAR A.A., NAFISAH S., MD SAAD S.K., TEE TAN S., BALOUCH A., MAT SALLEH M., OYAMA M., *Poriferous microtablet of anatase TiO₂ growth on an ITO surface for high-efficiency dye-sensitized solar cells*, Solar Energy Materials and Solar Cells **122**, 2014, pp. 174–182.

- [15] UMAR A.A., RAHMAN M.Y.A., SAAD S.K.M., SALLEH M.M., OYAMA M., *Preparation of grass-like TiO₂ nanostructure thin films: effect of growth temperature*, Applied Surface Science **270**, 2013, pp. 109–114.
- [16] UMAR A.A., OYAMA M., *Attachment of gold nanoparticles onto indium tin oxide surfaces controlled by adding citrate ions in a seed-mediated growth method*, Applied Surface Science **253**(5), 2006, pp. 2933–2940.
- [17] UMAR A.A., OYAMA M., *Growth of high-density gold nanoparticles on an indium tin oxide surface prepared using a “touch” seed-mediated growth technique*, Crystal Growth and Design **5**(2), 2005, pp. 599–607.
- [18] UMAR A.A., OYAMA M., *A cast seed-mediated growth method for preparing gold nanoparticle-attached indium tin oxide surfaces*, Applied Surface Science **253**(4), 2006, pp. 2196–2202.
- [19] KITYK I.V., MERVINSKII R.I., KASPERCZYK J., JOSSI S., *Synthesis and properties of nm-sized Sn₂P₂Se₆ single crystals embedded in photopolymeric host*, Materials Letters **27**(4–5), 1996, pp. 233–237.
- [20] KITYK I.V., PLUCINSKI K.J., EBOTHÉ J., UMAR A.A., OYAMA M., *Control of the plasmon absorption of gold nanoparticles with a two-color excitation*, Journal of Applied Physics **98**(8), 2005, article 084304.
- [21] OZGA K., KAWAHARAMURA T., UMAR A.A., OYAMA M., NOUNEH K., ŚLEZAK A., FUJITA S., PIASECKI M., RESHAK A.H., KITYK I.V., *Second order optical effects in Au nanoparticle-deposited ZnO nanocrystallite films*, Nanotechnology **19**(18), 2008, article 185709.
- [22] OZGA K., OYAMA M., SZOTA M., NABIALEK M., KITYK I.V., ŚLEZAK A., UMAR A.A., NOUNEH K., *Photoinduced absorption of Ag nanoparticles deposited on ITO substrate*, Journal of Alloys and Compounds **509**(Supplement 1), 2011, pp. S424–S426.
- [23] GRUHN W., KITYK I.V., BENET S., *Photoinduced optical second harmonic generation in Fe-Co metallic spin glasses*, Materials Letters **55**(3), 2002, pp. 158–164.
- [24] MAJCHROWSKI A., KITYK I.V., EBOTHÉ J., *Influence of YAB:Cr³⁺ nanocrystallite sizes on two-photon absorption of YAB:Cr³⁺*, Physica Status Solidi B **241**(13), 2004, pp. 3047–3055.

*Received December 29, 2014
in revised form January 20, 2015*